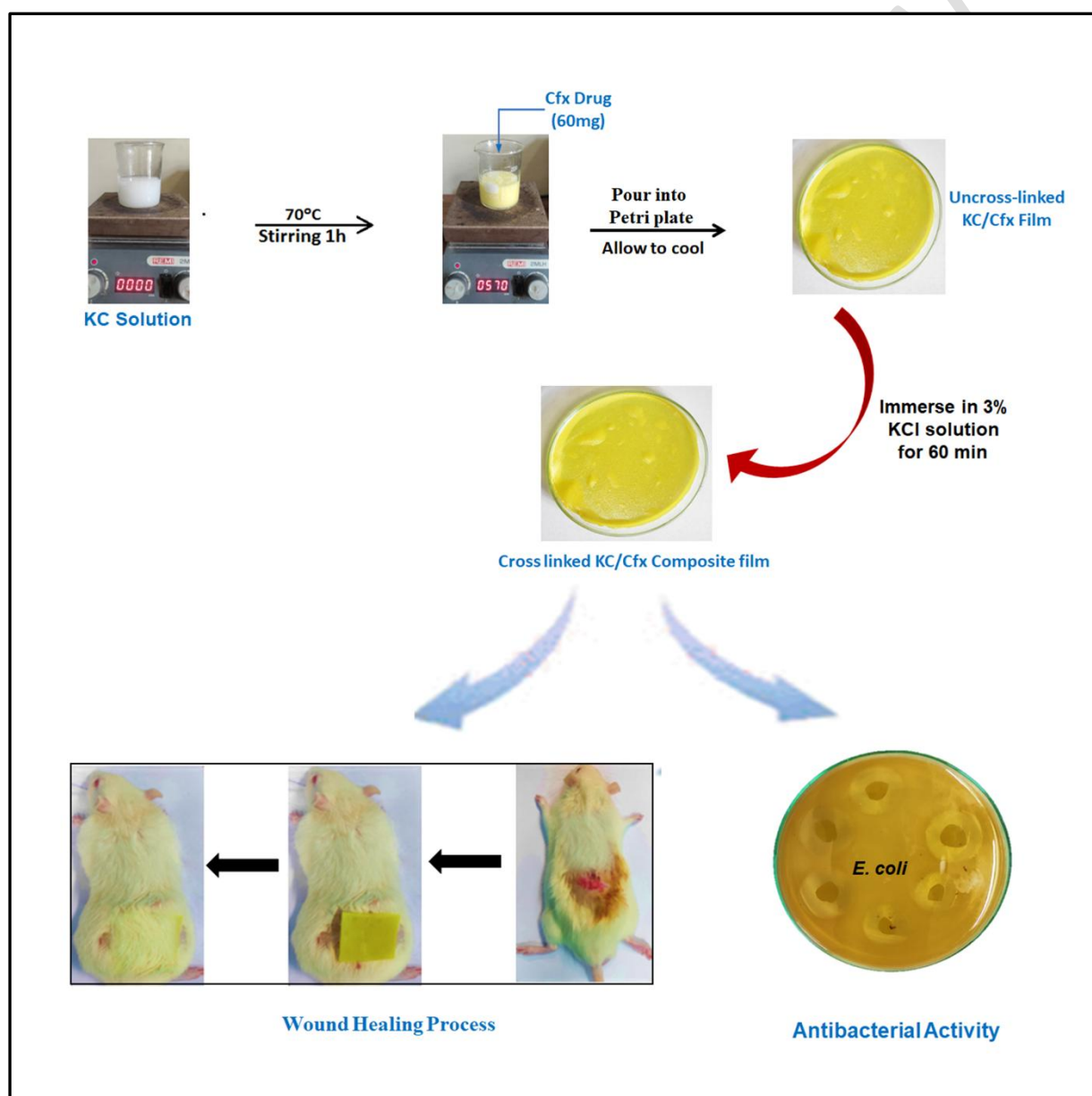


Kappa-Carrageenan/Ciprofloxacin loaded hydrogel patch for wound healing application

Graphical Abstract

Ciprofloxacin loaded Kappa Carrageenan films showed fair ability to treat bacterial infections on wounds. The animal studies, performed on rats, also established their strong candidature in the protection of wound from infection.



Graphical Abstract

Abstract

Kappa carrageenan/Ciprofloxacin composite films have been developed to protect wounds from bacterial infection. The films were characterized by FTIR, TGA, and SEM analysis. The Water Vapor Transmission Rates (WVTR) for film samples, with different compositions, was in the range of 1025 to 1181 g m⁻²day⁻¹. The O₂ permeability for the samples tested was 16.6 mg/mL against the values of 10 and 28 mg/mL obtained for negative and positive controls respectively. As compared to the standard moisture loss from wounded skin, the relatively low values indicated their suitability for low exudating wounds. The total release of drug Ciprofloxacin from the samples loaded with 0.06, 0.13 and 0.19 g drug/g gel was found to be 29.13, 71.75, 85.90 mg/g gel in the media of pH 7.4 and the time required for the release was almost 240, 320 and 356 min respectively. The release data were best interpreted by 'Power Function Model', as indicated by high regression values of 0.9793, 0.9862 and 0.9994 respectively. The release exponent 'n' values were 0.55, 0.33 and 0.42 respectively, thus suggesting a diffusion-controlled mechanism. The films showed fair antibacterial activity against model bacteria *E. Coli*. Finally, Kappa carrageenan/Ciprofloxacin composite films, when applied on artificially created wound on skin of rats, showed excellent healing with no inflammation and bacterial infection.

Key words: Carrageenan, wound dressing, drug release, Ciprofloxacin.

1. Introduction

Kappa Carrageenan (KC), is an anionic linear sulphated polysaccharide, consists of alternating α -1,3 galactose and β -1,4,3,6 anhydrogalactose with one sulphate ester groups [1]. Its viscoelastic and thermo-gelling property, and presence of many functional groups (sulphate and hydroxyl) make it a suitable candidate for biomedical applications [2-4]. The special property of KC to undergo thermal gelation makes it a better candidate for preparing hydrogel patch as compared to other biopolymers/synthetic polymers which require some chemical reactions to yield a stable hydrogel. In fact, KC has so many advantageous features: (i) it has wound healing property, (ii) it undergoes thermal gelation (iii) no toxic chemicals are required to prepare polymeric film, (iv) any bioactive ingredient can conveniently be incorporated into KC film just by mixing the ingredient into pre-gel forming solution under normal stirring, and finally, the stability of KC film can be enhanced by carrying out its ionic crosslinking using KCl. Recent past has witnessed tremendous research work on polysaccharides-based hydrogel patches that have been fabricated to manage wound healing process [5,6]. Thus, looking to the above highlighted properties of polymer Carrageenan, we hereby propose a hydrogel patch, composed of natural polysaccharide Kappa Carrageenan and an antibacterial drug Ciprofloxacin and this proposed hydrogel patch heals the wound in effective way by fighting against bacterial infection and enhancing the healing process.

2. Experimental

2.1 Materials

- *Kappa-Carrageenan (KC)*

Kappa-Carrageenan (Irish moss) with high molecular mass was purchased from Hi Media Chemicals, Mumbai, India and used as received.

- *Ciprofloxacin (Cfx)*

Ciprofloxacin fluoroquinolone antibiotic having molecular weight 331.346 g/mol was obtained from local medical store.

- *Potassium Chloride (KCl)*

Potassium Chloride, readily dissolves in water and having molecular mass 74.551 g/mol was purchased from Hi Media Chemicals, Mumbai, India and used as received.

- *CuticellTM*

CuticellTM Chlorhexidine Acetate is a commercial dressing (Batch no.21CC026), sterilised by gamma irradiation, bought from a local medical store.

- *Water*

The double distilled water was used in all the experiments.

2.2 Preparation of K⁺ Ions Crosslinked plain KC Film

50 ml of 1.6 % (w/v) solution of KC was taken in a beaker and to this 1 ml of glycerol was added under mild stirring at 70°C till a uniform transparent solution was obtained. Now, the above solution was poured into a Petri plate and allowed to cool. The resulting film, obtained due to the thermal gelation, was carefully removed and poured into 250 ml of a 3% (w/v) KCl solution for 60 minutes to allow the ionic crosslinking. The cross-linked film was dried in a dust-free chamber at room temperature.

2.3 Preparation of KC/Cfx Film

Hot aqueous solution of KC, containing definite quantities of drug Cfx, was poured into Petri plate and allowed to cool for thermal gelation to take place. The film was taken out carefully and immersed in 3% KCl solution (w/v) for 60 min to crosslink the film. The film was taken out, dried at 40°C and put in a dust-free chamber for further use. In **Fig.1**. Overall scheme for the preparation of composite film (KC/Cfx) is shown.

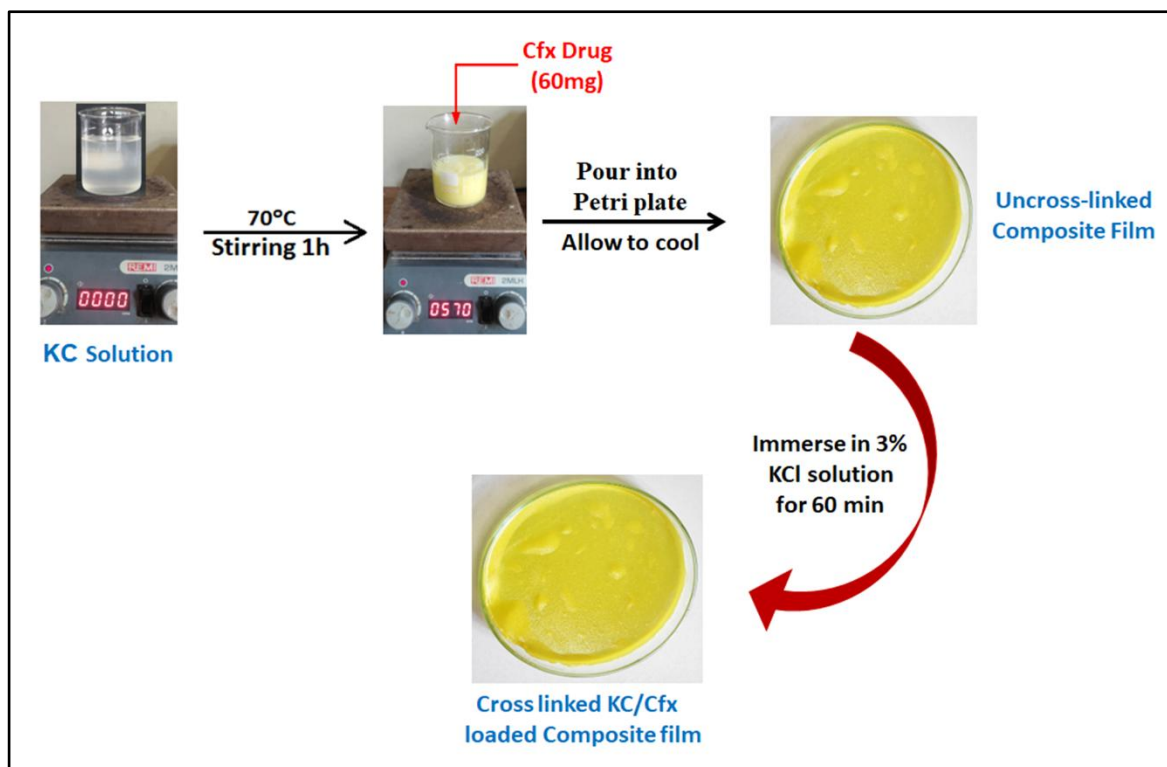


Fig.1. Overall scheme for the preparation of composite film.

Table.1. Composition of various films prepared

The representative sample is designated as: FCf_y
 F = 1.6% Kappa carrageenan cross-linked with 3%(w/v) KCl solution

Sample Code	Amounts of various Constituents		
	Carrageenan % (w/v)	Ciprofloxacin (g/g gel)	KCl % (w/v)
FCf _{0.00}	1.6	0.00	3.0
FCf _{0.06}	1.6	0.06	3.0
FCf _{0.13}	1.6	0.13	3.0
FCf _{0.19}	1.6	0.19	3.0

Where, the number *y*, in subscripts, denote the amount of drug Ciprofloxacin (in mg) present per g of film , symbol F represents a Carrageenan film composed of 1.6 % (w/v) film forming solution and 4 percent (v/v) glycerol and crosslinked with 3 %(w/v) of KCl solution.

2.4 Determination of Drug Entrapment Efficiency (DEE)

The concentration of the drug, leached out during the crosslinking process, was determined as follows: After the crosslinking was over, the film was taken out and the crosslinking solution was made up to its original volume and its absorbance was determined spectrophotometrically (Thermo, USA) at 390 nm. The absorbance was transformed into concentration using a pre-plotted Beer-Lamberts law. The DEE was determined using the following expression:

$$\text{DEE} = \frac{C_i - C_f}{C_i} \times 100 \quad \dots (1)$$

Where, C_i = Initial amount of drug added in the film-forming solution.

C_f = Amount of drug leached out in the cross-linker solution.

2.5 Characterization

2.5.1 FT-IR Analysis

The infrared spectrum of absorption of a solid is obtained by Fourier Transform Infrared Spectrophotometer (Shimadzu, 8400, Japan). The powdered form of plain K^+ ions crosslinked Carrageenan, Cfx loaded composite film samples were analysed. And powdered sample was mixed with KBr, the scan was recorded, and the selected spectral range was in between 400 to 4000 cm^{-1} .

2.5.2 SEM Analysis

The surface morphology of the plain K^+ ions crosslinked Carrageenan film and Cfx loaded composite film was determined by Scanning Electron Microscope analysis by using JEOL 6400 F microscope. The accelerating voltage of 2 KV and a working distance of 4.4 mm with a 50 μL sediment suspension were sprayed silicon wafers to clean them followed by air drying for 24 hours, and then being coated with an approximately 6 nm layer of gold and palladium.

2.5.3 Thermo-gravimetric Analysis

The thermal stability was determined by thermogravimetric analysis and was performed by using Thermo Gravimetric Analyser (Mettler, Teledo TGA/SDTA 851, and Switzerland). A small amount of grinded powdered sample was kept in a ceramic crucible and analysed under

the rate of flow of N₂ 30 ml/min and the temperature range of 30°C to 800°C, at the heating rate of 10°Cmin⁻¹.

2.6 Water Vapor Permeation Study

The water vapor transmission rate (WVTR), as determined by ASTM method E96-90, Procedure D, Briefly, After, taking initial weight of the test cups, were placed in incubator as soon as the cups were taken out at different time intervals and weighted correctly. The films were mounted at the circular opening of a permeation bottle. Water vapor transmission rate was calculated as [7]

$$\text{WVTR} = \frac{\Delta W}{\Delta t \cdot A} \text{g.h}^{-1}.\text{m}^{-2} \quad \dots (2)$$

Where, ΔW is the change in mass of cup in a time interval Δt and A is the surface area (πr²) of the film exposed to water vapor.

2.7 Moisture Sorption Study

By using gravimetric static method [8-10]. Before the moisture sorption experiments, the film samples are kept in an electric oven for two days at 40°C temperature to dry the samples. Completely saturated salt solutions were transferred into separate jars. The jar was filled with crystalline salt. At 37°C a pre-weight dried film samples collected and placed inside the desiccator contains the saturated salt solution. The jar was maintained in asanyo MTR 152 Incubator at 37°C for the equilibration of samples. The samples took about five days to reach equilibrium. The moisture contain of the equilibrated film sample was evaluated by using vacuum oven method. And the equilibrium moisture contain of the film samples was expressed as g/g dry solids and EMC was determined by using following formula-

$$\text{EMC} = \frac{\text{Final weight} - \text{Initial weight}}{\text{Initial weight}} \text{g/g} \quad \dots (3)$$

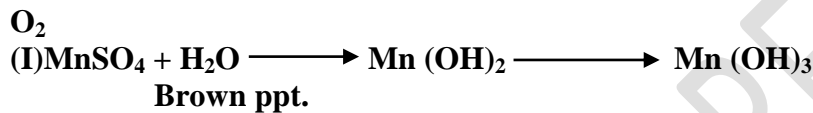
2.8 Oxygen Permeation Study

In oxygen permeation experiment the film samples were placed on the top of the conical flask. The conical flask contains 200 ml of de-ionised water. The positive control allowing

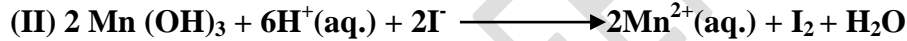
oxygen to enter the flask and dissolve in distilled water and it is open flask while the negative control was closed flask. All the flask with film samples including positive and negative control were placed in an open environment for 24 h.

The water in the flask was then analysed to evaluate the amount of dissolve oxygen using the Winkler Technique (step I- step III) [11]

Step I- First and foremost, 1ml of 3M MnSO₄ solution was added to the test samples followed by addition of 2ml alkaline solution (4ml KI and 3M KOH solution) without allowing any air to pass in test medium. A Pinky-brown precipitate emerged and was used for further analysis.



Step II- In the second step 1ml of sulphuric acid (50%) was added. The precipitate that appeared in the first step was completely dis dissolved and a clear solution was noticed.



Step III- By using 0.1% starch solution as indicator, 50 ml of clear solution obtained in the second step was stepped out in a titration flask and titrated against 0.018 M sodium thio-sulphate (hypo) solution.



The amount of Dissolve Oxygen in mg/L was determined by using the expression -

$$\text{Amount of Dissolve Oxygen} = \frac{V_1 \times N \times E \times 1000}{\text{Volume of sample}} \quad \dots (4)$$

Where,

V₁= Volume of sodium thiosulphate.

N = Normality of sodium thiosulphate.

E = Equivalent weight of oxygen.

2.9 Expansion Study

The expanse of expanding wound dressing film on wound area was analysed by measuring the change in diameter of the film samples. In short, in 100 ml of deionised water, added 4g of gelatine powder and dissolve at 85°C temperature under mild stirring until a clear solution was obtained. Then 30 ml of this solution was poured into Petri plate and allowed to cool at room temperature, overnight then on this gelatine surface placed the film samples with known diameter, and samples diameter was monitored regularly till the sample gained a constant diameter [12]. The expansion ratio (ER) represents as

$$\text{ER} = \frac{\text{Diameter at time } t \text{ (D}_t\text{)}}{\text{Initial diameter (D}_0\text{)}} \quad \dots (5)$$

2.10 Drug Release Study

A pre-weighed hydrogel films with different concentration of drug were placed in 20 ml of PBS of pH 7.4 at 37°C. The samples were taken out after definite time intervals and put in fresh buffer saline. The absorbance of the solutions were measured at 380 nm and transformed into concentration using pre-plotted Beer-Lambert's plot.

2.11 Antibacterial Study

The Antibacterial sensitivity of the film samples were investigated by Zone of inhibition method in which the pure culture of *E. coli* and Mueller Hinton Agar plates were prepared. A loop full of the culture was suspended in micro lit of sterile water and spread on the plate. The sample with plain crosslinked KC film and KC with drug loaded composite film, discs were cut and placed on the Petri plates and were incubated at 37°C for 24 h to observe results [13].

2.12 haemolysis

The test samples were analysed for its haemolytic properties using the method described in American Society for Testing and Materials. The experiment was carried out in (Avika Biological Research Foundation, Jabalpur). A sample with 1cm² area was dipped in 7 ml of 0.9% PBS solution at 37°C for the duration of 24 h. Now film was removed from PBS solution and 0.05ml blood was added on to its surface thereafter film was emerged in PBS solution and maintained for 3 h at 37°C, the above solution was centrifuged at 4000 rpm for 5 min. Positive, negative and blank control was prepared by adding same amount of ACD

blood to 10ml distilled water, 0.9% of PBS solution with Plain KC film and 0.9% of PBS solution respectively. And after incubation sample were transferred to separate disposable centrifuge tubes. All tubes were centrifuged for 15 min. By using a spectrophotometer, the absorbance of each supernatant of test sample, positive, negative control and blank was measured at 540 nm.

Abs.(sample) – Abs. (Blank)

$$\text{Blank corrected \% haemolysis} = \frac{\text{Abs.(sample) – Abs. (Blank)}}{\text{(Diluted blood) – Abs. (Blank)}} \times 100 \quad \dots (6)$$

2.13 Animal Study

2.13.1 Skin Irritation Studies

Standard skin irritation test in albino rats were also performed to evaluate any side effect of new therapeutic preparation Kappa-Carrageenan film & KC/Cfx loaded composite film. In brief, nine wistar albino rats, dorsal area of the trunk of the rats (4x4 cm²) were shaved aseptically 24 h before the test. Study protocol was approved by the IAEC. Rats were grouped two groups, containing three rats per group. As Kappa-Carrageenan patch and Carrageenan/ Cfx patch respectively. The skin of applied area was observed for at first 60 min. and then at 24-, 48- and 72-hours interval for any kind of skin reaction specially for erythema and oedema [14].

2.13.2 Animal Wound Healing Study

Study protocol was approved by the Institutional animal ethics committee (IAEC). Rats were divided into two treatment and one control groups (3 animals in each group).

- Group1: No treatment, allowed for natural healing.
- Group2: Applied Carrageenan patch (vehicle) on wounded area
- Group 3: Applied for Carrageenan/ Cfx patch.

A patch of 4X4cm² was applied on the wounded area and dressed with bandage. Observation of wounded area was done on day1, day 3, day 5, day 7 and day 10 and scored [15].

2.13.3 Histological Evaluation of Healed Wound

Representative samples of skin from the studied area were collected and preserved in 10 % formalin for paraffin histopathology. The processed tissue is embedded in the wax mould, followed by five-micron thin sections were taken on glass slide. These sections were stained with Haematoxylin and Eosin stain. Histopathological observations were recorded by observing the slides under Light microscope.

3. Result and Discussion

3.1. Preparation of K⁺ Ions Cross-linked Plain KC Film

When thermally gelled KC film is immersed in the KCl aqueous solution, K⁺ ions enter into the film matrix and occupy place within the double helical structures to counter the negatively charged sulphate groups. As the distance between the two-hydrogen bonded in double helices is almost 0.3 nm and the size of potassium ions is 0.26 nm, the approach of K⁺ ions is highly probable to occupy the junction points to produce cross linked matrix.

3.2 Preparation of Drug-loaded KC Film

When hot aqueous solution of KC, containing definite quantities of drug Cfx is poured into Petri plate and allowed to cool, thermal gelation takes place and drug loaded uncross linked KC/Cfx film is obtained. On immersion of this film into aqueous KCl solution, K⁺ ions inter into network and counter balance negative charges of sulphate groups that are present along the Carrageenan chains. First of all, K⁺ ions enter through the surface of film, simultaneously crosslinking KC chains present on the surface. As potassium ions penetrate further into the film matrix, they continue to produce crosslinked structure throughout the film matrix. As the surface was crosslinked first, leaching of drug was very low, hardly 2.8 to 4.6 percent.

3.3 Characterization

3.3.1 FT-IR Analysis

In FTIR spectrum of sample FCf_{0.0}(KCl cross linked KC film), **Fig.2. (a)** a peak at 1010 cm⁻¹ confirms the glycosidic linkage and band at 1270 cm⁻¹ is ascribed to the sulphate group. The OH stretching vibration is also observed in the region of 3000cm⁻¹ to 3600cm⁻¹. The FTIR spectrum of composite film KC/Cfx (FCf_{0.13}), shown in **Fig.2. (b)**, the characteristic broad peak of Cfx is found at 1650 to 1600 cm⁻¹ which is assigned to quinolones, a band appearing

at 1010cm^{-1} indicates the presence of glycosidic bond which are also present in spectrum of KC.

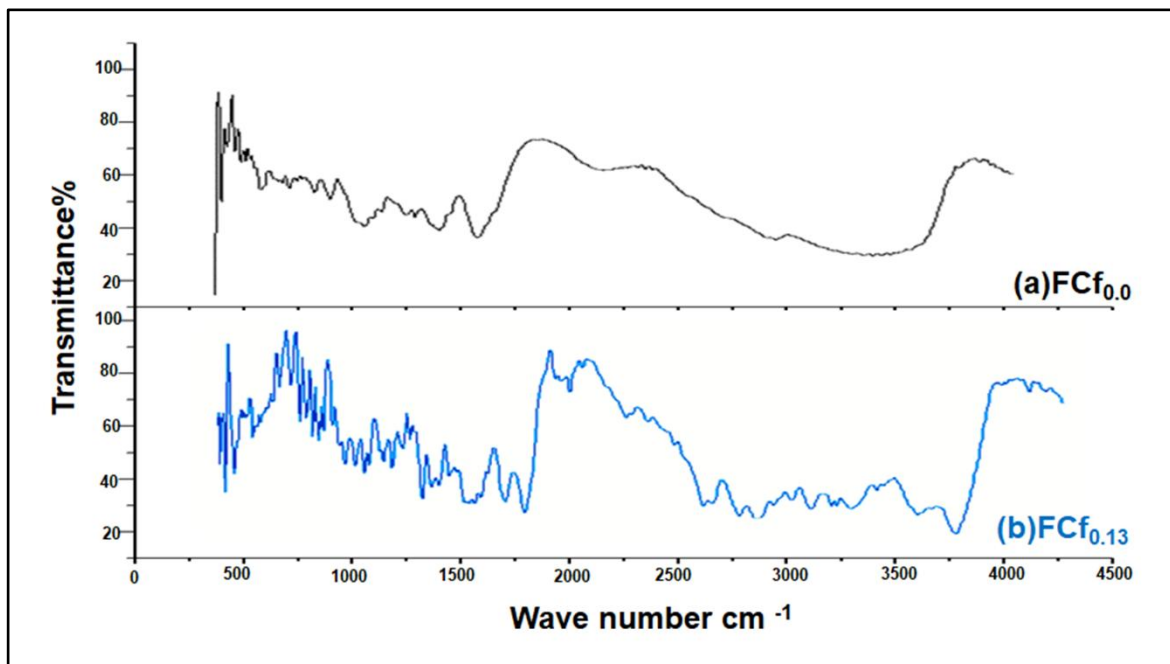
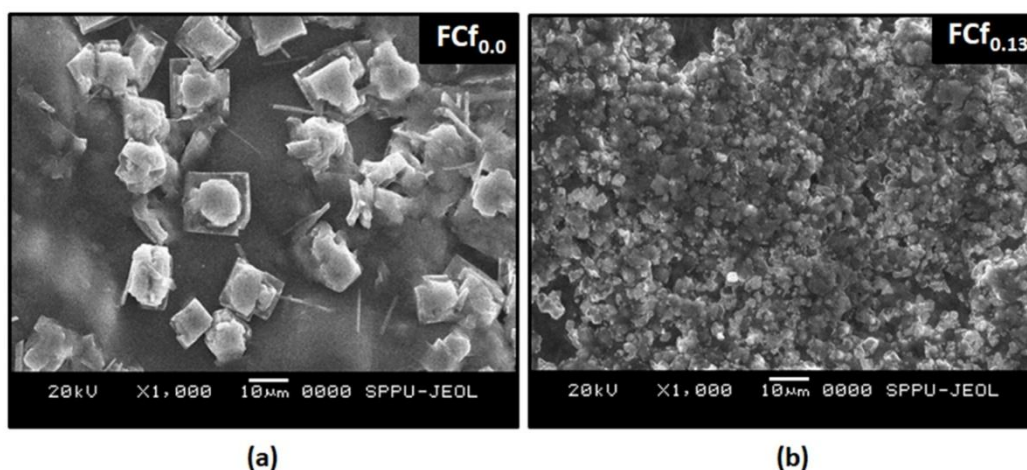


Fig.2. FTIR spectra of (a) Plain KCl crosslinked KC film $\text{FCf}_{0.0}$ and (b) drug loaded composite film $\text{FCf}_{0.13}$ (Defence Institute of Advance Technology, Pune).

3.3.2 SEM Analysis of Film Samples

The SEM images of samples $\text{FCf}_{0.0}$ and $\text{FCf}_{0.13}$ with 1000 X magnifications are shown in **Fig.3. (a)** and **(b)** respectively. It can clearly be seen in **Fig.3. (a)** that plain KC film contains aggregated Carrageenan particles distributed uniformly throughout the matrix. The observed agglomerations may be due to some partially dissolved KC particles. The surface texture of drug loaded film, as shown in **Fig.3. (b)**, reveals presence of uniformly dispersed Cfx.



(a)

(b)

Fig.3. SEM Images of (a) Plain KCl crosslinked Carrageenan film FCf_{0.0} and (b) drug loaded composite FCf_{0.13} (Defence Institute of Advance Technology, Pune).

3.3.3 TGA Analysis of Film Samples

The Fig.4. (a),(b) and (c) show TGA of samples FCf_{0.0}, native drug Cfx and sample FCf_{0.13} respectively. The sample FCf_{0.0} shows a weight loss by 17% when heated up to 250°C, probably due to moisture evaporation. Furthermore, around 13% more weight loss occurs from 250 to 800°C, due to the partial degradation of Carrageenan polymeric backbone. It is worth mentioning that a weight loss of 69% for native Carrageenan, when heated to 500°C, has been reported [16]. This clearly indicates that crosslinking by K⁺ ions enhance the stability of the film. The TGA profile of the sample FCf_{0.13} shows minimum stability as compared to its components. There is 20% weight reduction up to 200°C, associated with moisture loss, followed by a drastic weight loss up to 800°C. This indicates that presence of drug Cfx within film matrix causes a severe loss in the stability of film. The reason is that presence of drug molecules reduces the electrostatic attraction between K⁺ ions and Carrageenan, thus lowering the degree of crosslinking and so thermal stability.

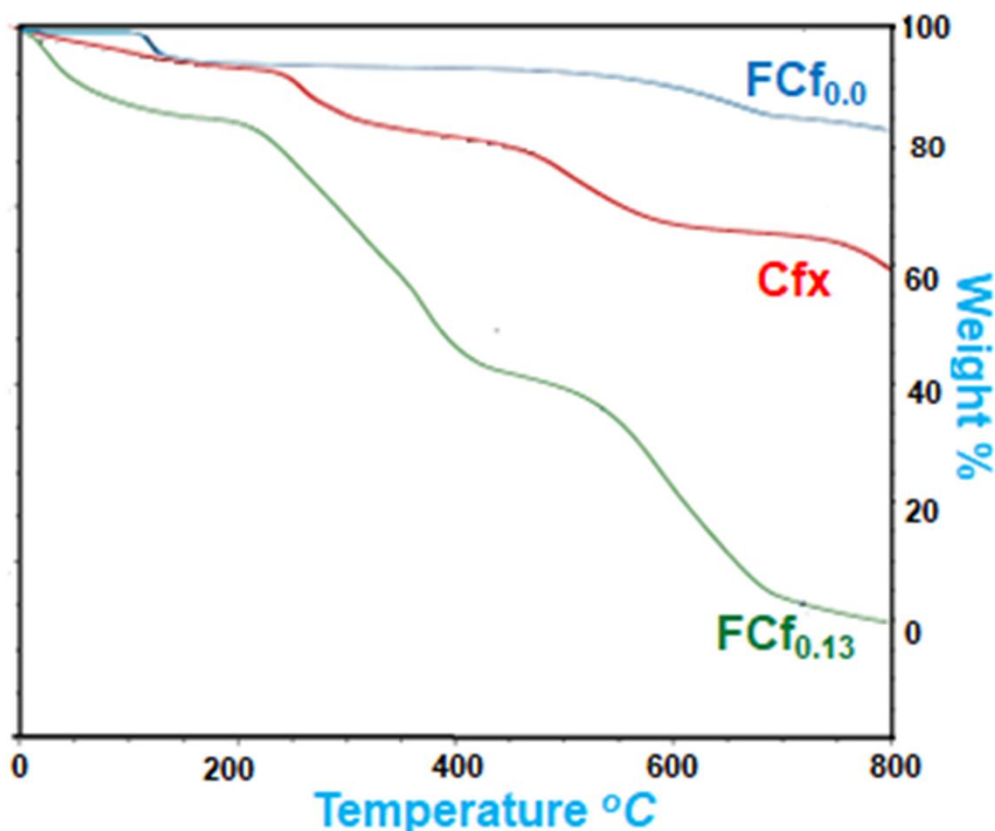


Fig.4. Thermo-gravimetric analysis curves of (a) Plain KCl crosslinked KC film FCf_{0.0}, (b) drug Ciprofloxacin and (c) Composite film FCf₀.

3.4 Water Vapor Transmission Studies

When a dressing, with high WVTR, is placed over a wound, water vapor may transmit through it at a faster rate, thus making wound surface dry, which may lead to slow healing. On the other hand, a wound dressing with low WVTR may not be able to transmit moisture at faster rate from the high exudating wound, thus leading to accumulation of exudate below the dressing. In the present work, WVTR was determined for the samples with different drug loading (FCf_{0.06}, FCf_{0.13} and FCf_{0.19}) The results are shown in **Fig.5.(a)** and different crosslinkers content (F (0)Cf_{0.13}, F (1) Cf_{0.13}, F (3)Cf_{0.13}, The results are shown in **Fig.5.(b)** along with a commercial dressing as reference. It is clear from the **Table 2** that WVTR for all types of film samples is in the range of 1025 to 1181 g m⁻²day⁻¹. This indicates that WVTR values of films are not dependent on their composition. The low WVTR values, thus obtained, may be due to (i) presence of drug molecules within the matrix, who put hindrance in diffusion of vapor through film, (ii) the H-bonded double helices and drug Cfx molecules render a nonporous texture to the films. So, lack of porosity retards the rate of diffusion of vapor molecules. Since KC is a linear polysaccharide with one sulphate group per two galactose molecules, even 1% KCl solution is enough to produce fully crosslinked film because of limited sites. This may be the reason that higher KCl concentration does not alter degree of crosslinking and hence WVTR values (**Table 2**). The WVTR values of normal and injured skin are from 204gm⁻²day⁻¹ and 280gm⁻²day⁻¹ for a first degree burn respectively. Moreover, for a granulating wound it is 5140 g m⁻²day⁻¹ [17] According to reports, normal WVTR for dressings should range from 70 to 9400 g/m²/day. It appears that all the films studied in this work, have low WVTR and are suitable for low exudating wound. Moreover, commercial dressing, used in this study has WVTR of 384 g/m²/day only. Indeed, there is great variation in WVTR of commercial wound dressings. For example, WVTR values of 83.2, 792.0, 1296, 3350.4 and 4992.0 g/m²/day have been reported for commercial dressings Dermiflex, OpSite, Hydrofilm, Beschitin and Omiderm respectively. **Table 2** showing value of WVTR for the various samples synthesized.

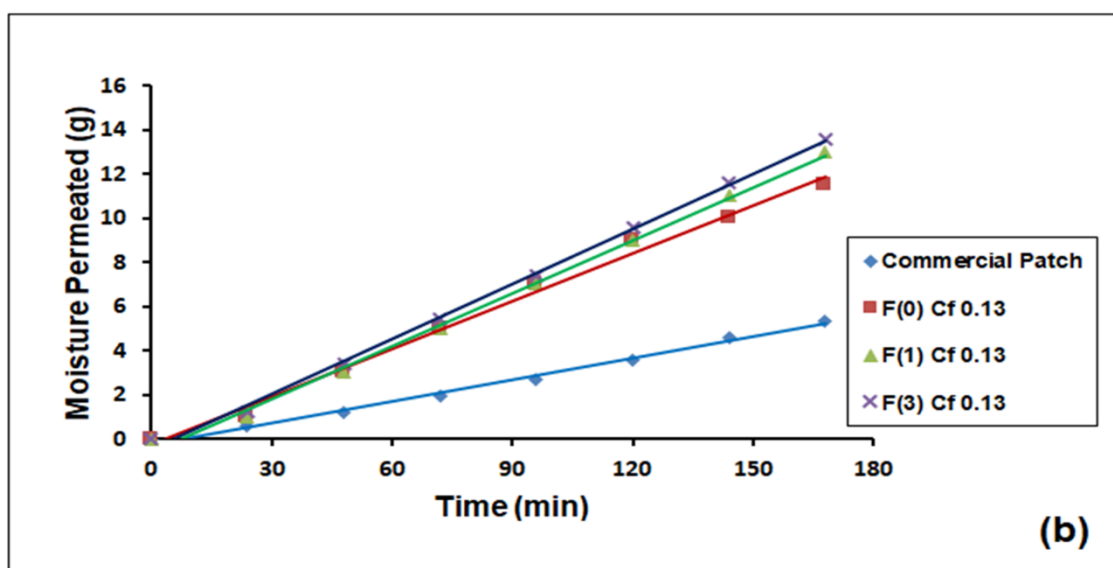
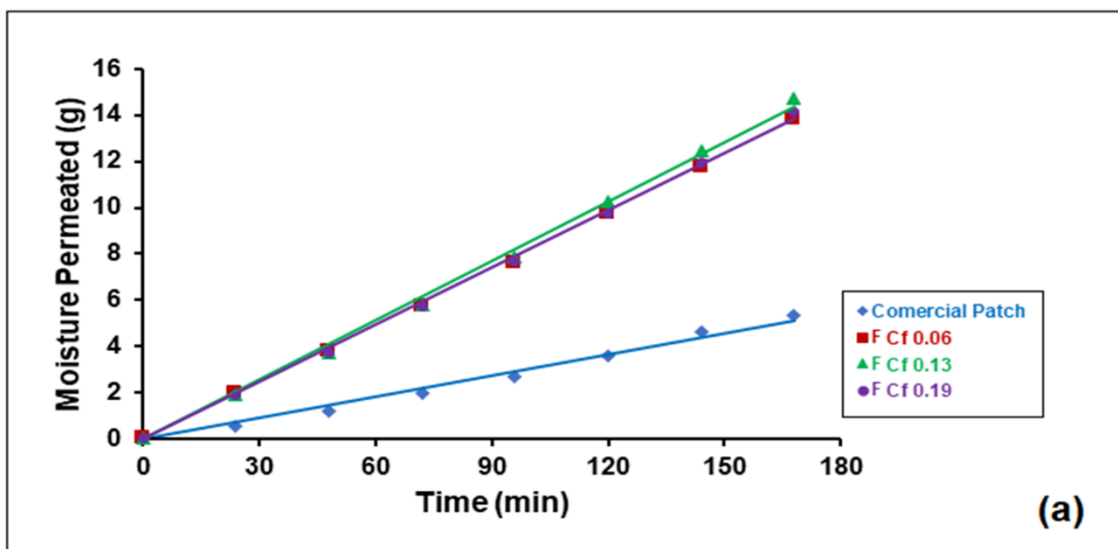


Fig.5. Kinetics of water vapor permeation through various films at 37°C.

Table. 2. Data showing parameters related with water vapor transmission rate for the various samples synthesized.

Samples	Moisture permeation parameter	
	WVTR ($\text{g.h}^{-1}.\text{m}^{-2}$)	WVTR ($\text{g.day}^{-1}.\text{m}^{-2}$)
Commercial patch	16.01	384.05
FCf _{0.13}	45.05	1081.24
FCf _{0.06}	42.73	1025.66
FCf _{0.19}	43.31	1039.56
F(0)Cf _{0.13}	44.12	1056.37
F(1)Cf _{0.13}	44.12	1056.37
F(3)Cf _{0.13}	48.07	1159.20

3.5 Moisture Sorption Study

The moisture uptake behaviour of samples FCf_{0.0} and FCf_{0.13} under varying water activity of environment are shown in **Fig.6**. In order to interpret the data in qualitative manner the whole relative humidity can be divided into three Zones that is Zone I with water activity up to 0.2, Zone II with a_w in 0.2 to 0.7 range and finally Zone III with a_w between 0.7 and 1.0

It is clear from the figure that there was almost negligible moisture sorption in Zone I which indicates there are strong molecular interaction present on the surface of the films.

The Zone II, known as multilayer sorption region indicate appreciable moisture sorption by the samples FCf_{0.0} and FCf_{0.13}. The reason is that in the given range 0.2 to 0.7 moisture is absorbed not only on the surface but also there is unfolding of polymeric chains, which offers new active sites for binding of water vapour molecule.

Finally, the moisture sorption in Zone III reveals some different trends; there is continuous increases in moisture sorption for sample FCf_{0.0} and it shows appreciable moisture uptake. This may be explained in the basis of fact that in this region, which is called condensation Zone, water vapour molecules enter into bulk of the film through voids and capillaries present within film matrix. However, sample FCf_{0.13} which had shown highest moisture uptake in Zone II, does not show any further increase in Zone III. This may probably due to the fact that the presence of drug molecules fills all the capillaries and voids

and therefore capillary action is not operative so effectively in Zone III. As a result, there is marginal moisture uptake in Zone III.

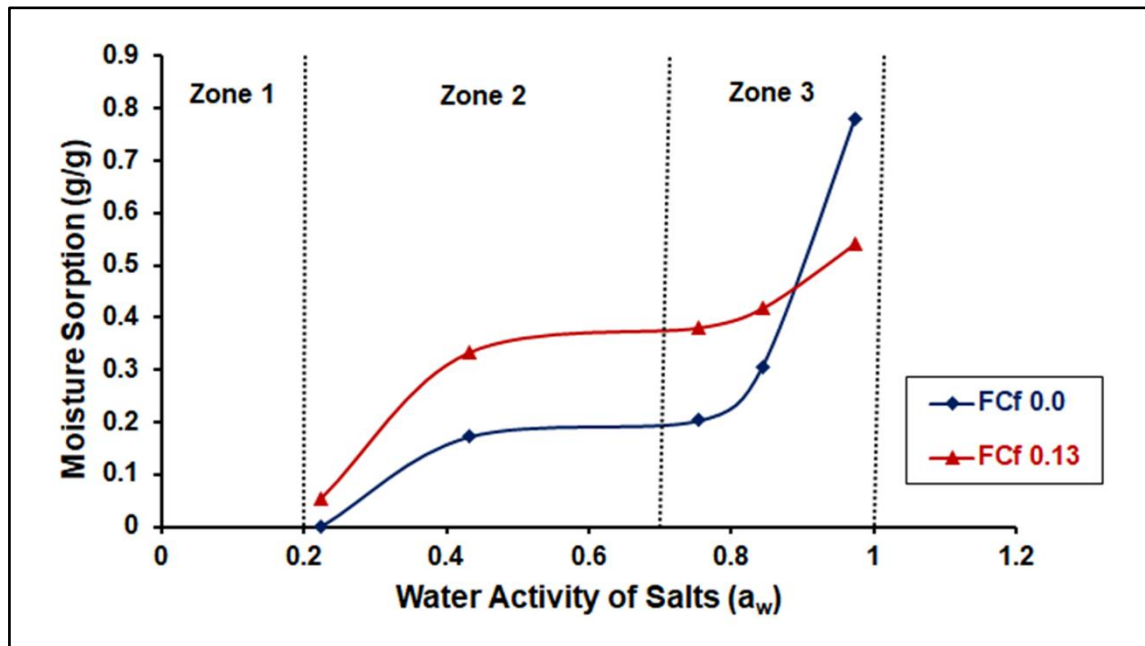


Fig.6. Showing moisture sorption by hydrogel films in environment of different water activities at 37°C.

3.6 Oxygen Permeation Study

The oxygen gas is required for tissue homeostasis, energy production, cell membrane maintenance, mitochondrial function and cellular repair therefore wound dressing films must have acceptable permeability for oxygen gas. The oxygen gas through the hydrogel film samples was achieved by measurement the dissolve oxygen in the distilled water using the Winkler Technique described in the experimental section, in which dissolve oxygen was expressed in milligram/ L unit. The dissolved oxygen value of purified water in the range of 10-30 mg/L at 37°C. The airtight negative flask and open positive flask for tested solution had Dissolve oxygen (DO) 10 mg/L and 28 mg/L respectively. The result of O₂ permeability for the hydrogel films in Bar diagram shown in **Fig.7**.

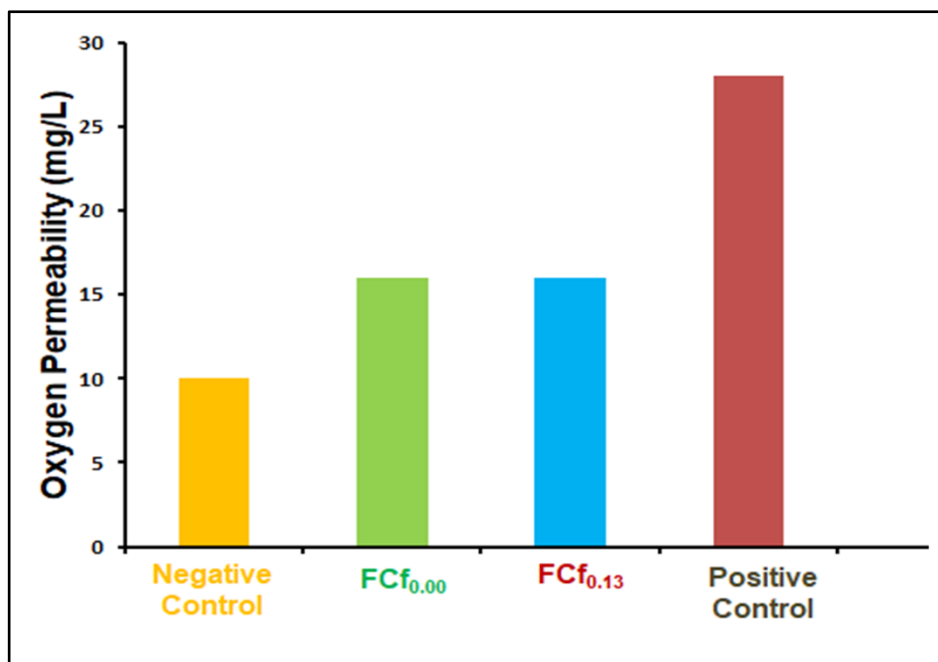


Fig.7. Bar diagram of O₂ permeability for the hydrogel films at 37°C.

3.7 Expansion Study

Fig.8. shows variation in diameter ratio D_t/D_0 with time for the samples. It is clear that the D_t/D_0 does not increase noticeably with time, thus indicating that the diameter of circular film, when placed in 4% gelatine solution, does not show any appreciable change. This observation is in the favour of wound healing patch because the increasing diameter may cause inconvenience to the patient and there are more chance of its detachment. However, in the present study the circular patch remains almost constant with respect to its diameter and hence it may be an additional favourable point for our proposal hydrogel patch.

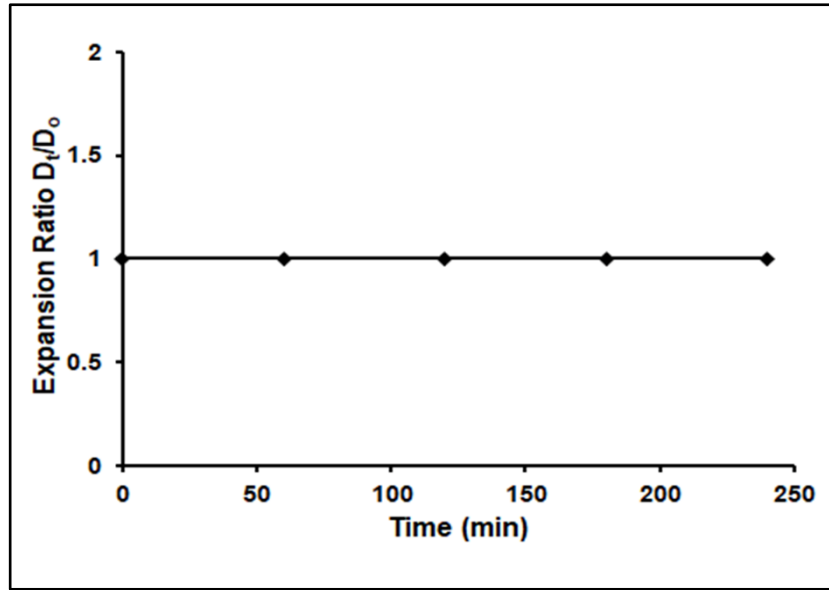


Fig.8. Showing expansion behaviour of the plain KC film $FCf_{0,0}$ and Cfx loaded composite film $FCf_{0,13}$ at $37^\circ C$.

3.8 Drug Release Study

The dynamic drug release profiles for the samples $FCf_{0,06}$, $FCf_{0,13}$ and $FCf_{0,19}$ in the PBS of pH 7.4 at $37^\circ C$ are shown in **Fig. 9(a)**. The three samples released approximately 29.13, 71.75, and 85.90 mg/g gel in 240, 320 and 356 min respectively. The drug release data were interpreted in terms of various kinetic models. For 'Power Function Model' graphs were plotted between $\ln M_t/M_\infty$ and $\ln t$ which were linear as shown in **Fig. 9. (b)**. The regression values, obtained, were fairly high (0.9773 to 0.9994) thus indicating the suitability of this model. The release exponent 'n' was found in the range of 0.3386 to 0.5523, thus revealing a 'diffusion controlled' mechanism for drug release (see **Table 3**). The reason is that H-bonded double helices and ionic crosslinking by K^+ ions may restrict chains relaxation and drug was only released due to diffusion process.

According to Schott model [18,19], drug release rate at any time is directly proportional to the quadratic of the quantity of drug left in the hydrogel before the attainment of equilibrium state. Mathematically:

$$d M_t/dt = k_2 (M_\infty - M_t)^2 \quad \dots (7)$$

The integration yields

$$t/M_t = 1/ k_2 M_\infty \quad \dots (8)$$

The t/M_t versus 't' plots for the films FCF_{0.06}, Cf_{0.13}, and Cf_{0.19}, are shown in **Fig.9 (c)**.

The linear nature of the plots enabled us to calculate the Schott kinetic rate constant

$$k_2 = \frac{\text{slope}^2}{\text{Intercept}} \quad \dots (9)$$

In addition, theoretical value of M_∞ was calculated using the following formula:

$$M_{\infty(\text{theor})} = \frac{1}{\text{slope}} \dots (10)$$

Poor regressions values (0.9630 to 0.9793) indicated that this model was less suitable.

Moreover, it was observed that there Was poor agreement between $M_{\infty(\text{theor})}$ and $M_{\infty(\text{exp})}$ values differed appreciably (**Table 3**).

We also used Beren-Hopfenberg model to interpret the release data. According to this model, rate of drug release at any time is proportional to the first power of the quantity of drug to be released till attainment of equilibrium. A plot between $\ln(1 - M_t/M_\infty)$ and 't' is shown in **Fig.9. (d)**.

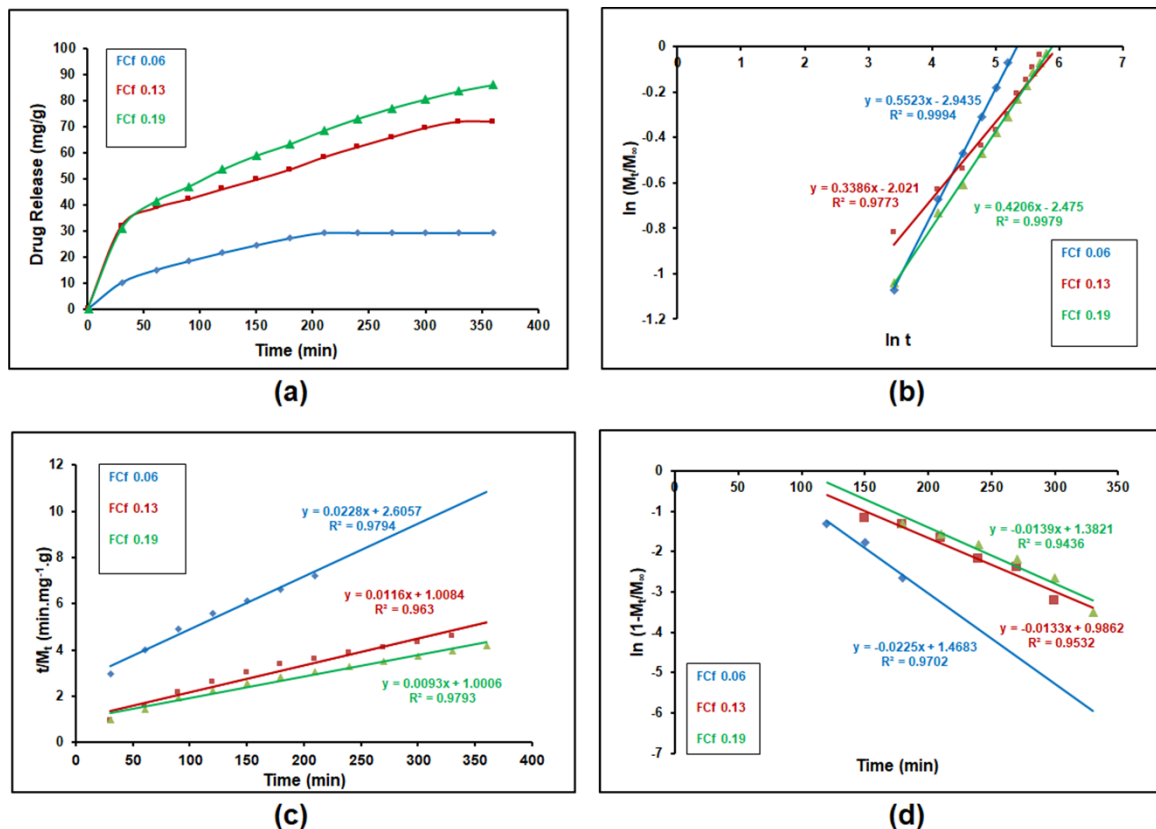


Fig.9 (a)Dynamic release of Cfx from various film sample in PBS of pH 7.4 at 37°C, (b)Power function model, (c)Scott model and (d)Beren-Hopfenberg model to interpret drug release data.

Table.3. Values of kinetic parameters obtained for different kinetic models in drug release experiments.

Samples	Power Function Model			Schott Model				Beren-hofenberg Model		
	n	$k \times 10^3$	R^2	$M_{\infty(th)}$ mg/g	$M_{\infty(ex)}$ mg/g	$k_2 \times 10^4$	V_{ini}	D_i	$k \times 10^3$	Ln A
FCf _{0.06}	0.55	1.13	0.99	43.85	29.13	1.99	0.38	3.61×10^{-5}	22.50	4.34
FCf _{0.13}	0.33	9.52	0.97	86.20	71.75	1.33	0.99	2.53×10^{-5}	13.50	2.68
FCf _{0.19}	0.42	3.34	0.99	107.90	85.90	8.64	0.99	2.44×10^{-5}	13.90	3.98

3.9 Antibacterial Study

The results (see Fig.10.) clearly indicate that the native Carrageenan film FCf_{0.0} shows a dense population of bacterial colonies (Fig.10. (a)). The Petri plate supplemented with drug-loaded film sample FCf_{0.13} exhibits a zone of inhibition (Fig.10. (b)) with average diameter of 20.33 mm, thus showing its optimal action against *E. Coli*.

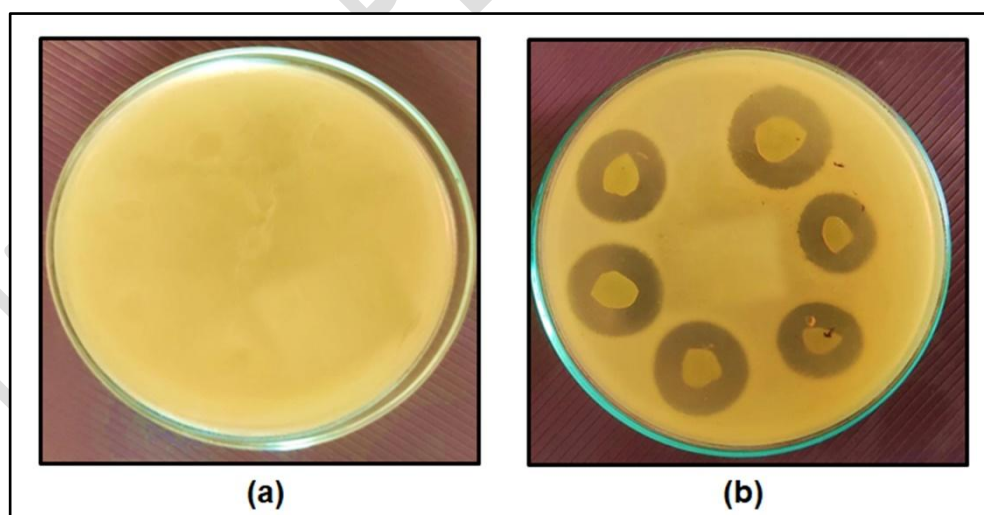


Fig.10. Growth of bacterial colonies in Petri plates supplemented with sample (a)FCf_{0.0} and(b)FCf_{0.13}at 37°C (Avika Biological Research Foundation, Jabalpur)

3.10 Haemolytic Test

Haemolytic test is considerable for wound dressing. Here the liberation of haemoglobin into plasma is investigated in this test which is caused by breakdown of erythrocyte membrane. The haemolytic index of the test sample FCf_{0.13}, is 1.006 % which is <2% there for the sample is non-haemolytic [20].

3.11 Animal Study

3.11.1 Skin Irritation Study

Results of the present study showed there was no skin reactions especially the erythema, haemorrhage and oedema were noted on application of these patches. Hence, concluded that this newly developed the rapeutic patch did not produce skin irritation in rats and quite safe for application.

3.11.2 Wound Healing Observation

On day 3, wounded area of rats of group 1 and 3 showed initiation of healing process, in terms of dryness and brown coloration of haemorrhage (**Fig.11.(a), (c)**). Rats of group 2 showed swollen and moderate inflamed wounded area.

On day 5, the wound healing was considerably more in the animals which were applied with gel patch containing Cfx (group 3) compared to group 1 animals. As shown in (**Fig.11. (c) & (a)**)Whereas rats applied with plain Carrageenan KCl crosslinked gel showed worsening condition, as inflammation, exudation and pus formation. Shown in **Fig.11.(b)**.

On the 10thday, wound of rats applied with KC/Cfx patch was healed approximate completely followed by group 1. As shown in (**Fig.11. (c) & (a)**) while in **Fig.11. (b)**, group 2 rats had worsened condition as pus exudation on wounded area. The above observations have also been tabulated in **Table 4**.

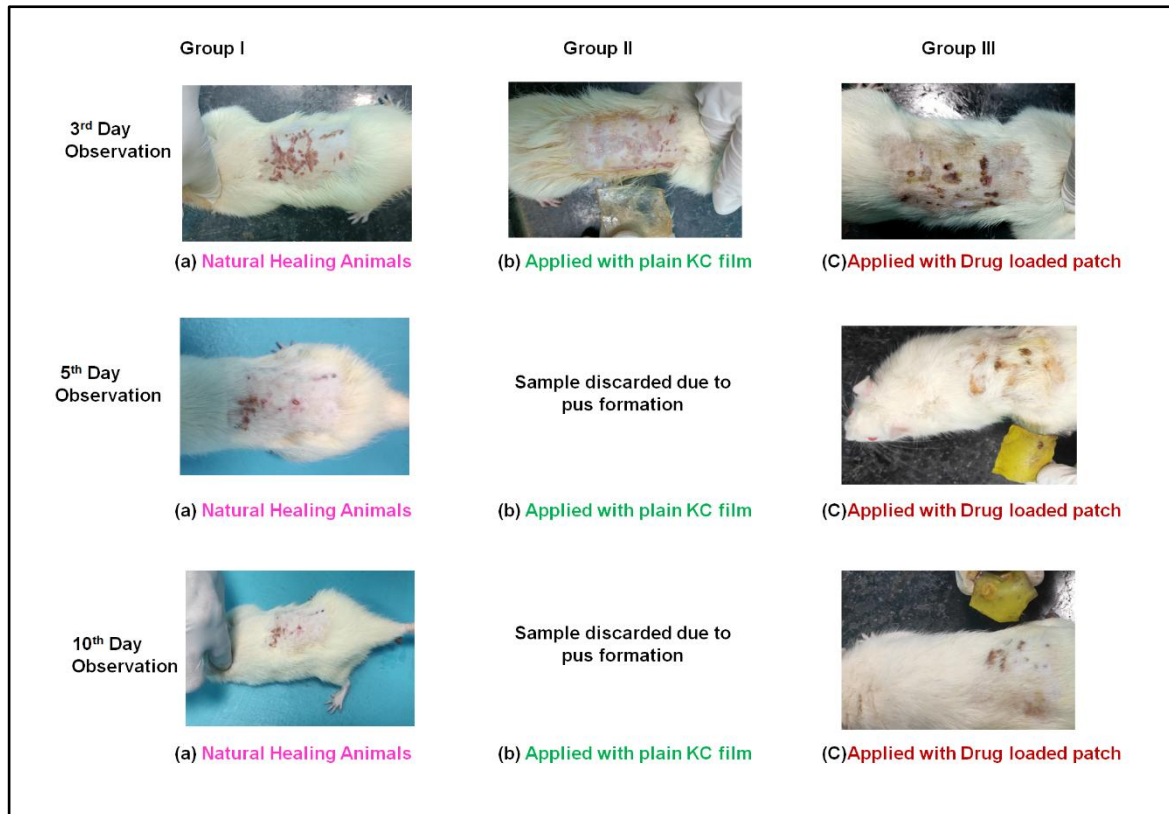


Fig.11.(Day 3) Haemorrhage and minimal inflammation in wounded area of group 1, inflammation and exudation in group 2, dryness and no inflammation in group 3. (Day 5) dryness and formation of scab in wounded area of group 1, sample discarded due to pus formation in group 2, partial closing of skin epithelium on wounded area along with hair growth in group 3. (Day 10) Partial irregular closing of skin epithelium and little hair growth in wounded area of group 1, regenerated upper layer of skin and moderate hair growth showed quite good healing of wounded area in group 3 at 37°C, (Govt. Veterinary Hospital, Jabalpur).

Table. 4. Observations of wound healing experiments on rates.

Observation day	Group 1	Group 2	Group 3
Day 0	Erythema (2) Haemorrhage (2)	Erythema (2) Haemorrhage (2)	Erythema (2) Haemorrhage (2)
Day 1	Haemorrhage (2) Inflammation (1)	Inflammation (2) Exudation (1)	Haemorrhage (2) Inflammation (0) Dryness (3)
Day 3	Haemorrhage (1) Inflammation (1) Dryness of wound (1)	Inflammation (3) Oedema (02) Exudation (3)	Formation of scab on wound (2)
Day 5	Haemorrhage (1) Dryness of wound (1) Formation of scab on wound (1)	Inflammation (3) Exudation (4) Pus (1)	Initiation closing of skin epithelium on wounded area (2) Partial hair growth (1)
Day 7	Initiation closing of skin epithelium on wounded area (1)	Inflammation (4) Pus (3)	Partial closing of skin epithelium on wounded area Hair growth (2)

Day 10	Partial irregular closing of skin epithelium on wounded area (1) Hair growth (1) Crust	Inflammation (4) Pus (4)	Healing of wound- (3) Hair growth (3)
--------	--	---------------------------------	--

3.11.3 Histological Evaluation

Histopathological examination of skin revealed, complete regeneration of epithelium of epidermis on wounded area as continue layer, keratinization and fibrous layer with growth of hair, near to normal skin histology in rats of group 3. Skin of group 1 Rats also showed regeneration of epithelium with epithelial hyperplasia and fibrosis (**Fig.12. (a), and (c)**) Rats of group 2 showed discontinued epithelial layer, eosinophilic exudation and micro abscessation, as evident by necrosis of epithelium and neutrophilic infiltration (**Fig.12.(b)**).

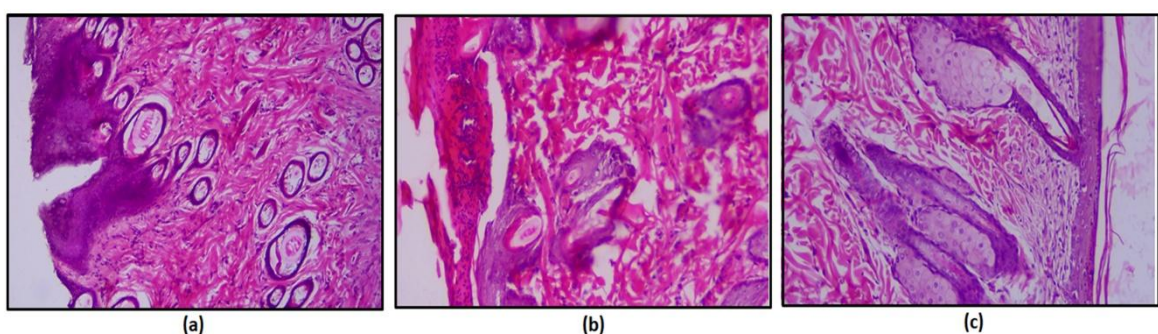


Fig.12. Microscopic section of skin of rats showing (a) epithelial hyperplasia in wounded area of group 1, (b) discontinued epithelium, necrosis and neutrophilic exudates in group 2 and (c) completely regenerated epithelium of group 3, H&E X100, at 37°C (Govt. Veterinary Hospital, Jabalpur).

4. Conclusion

It may be concluded from the above study that Ciprofloxacin/kappa carrageenan composite film offers its potential candidature to heal bacterial infected wounds. The moisture transmission rate, being low, makes this hydrogel patch suitable for low exudating wounds. The effective duration of drug release was almost 6 h, thus suggesting that it needs to be

replaced after every six hours. The antibacterial test, carried out on rats, also prove that this composite film is quite successful in wound healing.

7. Ethical approval statement

We hereby declare that approval was granted to carry out experiments involving human tissue by an ethics committee.

8. References-

- [1] Y. Sun, B. Yang, Y. Wu, Y. Liu, X. Gu, H. Zhang, C. Wang, H. Cao, L. Huang, Z. Wang, *Food Chemistry*. **178**, 311, (2015) <https://doi.org/10.1016/j.foodchem.2015.01.105>
- [2] S. Shen, X. Chen, Z. Shen, H. Chen, *Pharmaceutics*. **13**, 1666, (2021) [doi: 10.3390/pharmaceutics13101666](https://doi.org/10.3390/pharmaceutics13101666).
- [3] Z. Noralian, M.P. Gashti, M. R. Moghaddam, H. Tayyeb, I. Erfanian, *IntJBiolMacromol*. **180**, 439, (2021) <https://doi.org/10.1016/j.ijbiomac.2021.02.204>.
- [4] L. Madruga, K.C. Popat, R.C. Balaban, M.J. Kipper, *Carbohydrate Polymer*. **273**, 118541, (2021). <https://doi.org/10.1016/j.carbpol.2021.118541>.
- [5] M. Arab, M. Jallab, M. Ghaffari, E. Moghbelli, & R. Saeb, *Iranian Polymer Journal*. **30**, 1019–1028, (2021). [doi:10.1007/s13726-021-00952-7](https://doi.org/10.1007/s13726-021-00952-7).
- [6] S. Feiz, A.H. Navarchian, & O.M. Jazani, *Iranian Polymer Journal*. **27**, 193, (2018). [DOI:10.1007/s13726-018-0600-2](https://doi.org/10.1007/s13726-018-0600-2).
- [7] X.L. Shen, J.M. Wu, Y. Chen, *Food Hydrocolloids*. **24**, 285, (2010) [DOI:10.1016/j.foodhyd.2009.10.003](https://doi.org/10.1016/j.foodhyd.2009.10.003).
- [8] T.P. Labuza, *American Association of Cereal Chemist*. **29**, 92, (1984) <https://doi.org/10.1002/food.19850290122>.
- [9] E. Ayranci, and O. Duman, *Journal of Food Engineering*. **70**, 83, (2005) <https://doi.org/10.1016/j.jfoodeng.2004.08.044>.
- [10] F. Kaymak-Ertekin, *Lebensmittel- Wissenschaft and Technology*. **37**, 429, (2004) <https://doi.org/10.1016/j.lwt.2003.10.012>.
- [11] L.W. Winkler, *Chem. Ges.* **21**, 2843, (1888) [DOI:10.1002/CBER.188802102122](https://doi.org/10.1002/CBER.188802102122).
- [12] K.H. Matthews, *International journal of Pharmaceutics*. **289**, 51, (2005) [doi: 10.1016/j.ijpharm.2004.10.022](https://doi.org/10.1016/j.ijpharm.2004.10.022).
- [13] S. Park, P.S. Murthy, S. Park, Y.M. Mohan, and W. Koh, J. *Industrial and Engineering Chem.* **17**, 293, (2011) <https://doi.org/10.1016/j.jiec.2011.02.026>.
- [14] W. Feng, Z. Wang, *Carbohydrate Polymers*. **294**, 119824, (2022) <https://doi.org/10.1016/j.carbpol.2022.119824>.
- [15] S.K. Bajpai, S. Ahuja, N. Chand, M. Bajpai, *Int J BiolMacromol*. **104**(Pt A), 1012, (2017) [DOI: 10.1016/j.ijbiomac.2017.06.096](https://doi.org/10.1016/j.ijbiomac.2017.06.096).
- [16] M. Sadeghi, *Brazilian Journal of Chemical Engineering*. **29**, 295, (2012) <https://doi.org/10.1590/S0104-66322012000200010>.

- [17] H. Vrbanac, J. Trontel, S. Berglez, B. Petek, J. Opara, R. Jereb, D. Krajcar, I. Legen, EurJPharm Biopharm.**149**, 113, (2020)[DOI: 10.1016/j.ejpb.2020.02.002](https://doi.org/10.1016/j.ejpb.2020.02.002).
- [18] S.K. Bajpai, M. Jadaun, M. Bajpai, P. Jyotishi, F.F. Shah, S. Tiwari, IntJBiolMacromol.**104(PtA)**, 1064, (2017)[DOI: 10.1016/j.carbpol.2016.07.019](https://doi.org/10.1016/j.carbpol.2016.07.019).
- [19] S.K. Bajpai, V. Pathak, B. Soni, IntJBiolMacromol.**79**, 76, (2015).<https://doi.org/10.1016/j.ijbiomac.2015.04.060>.
- [20] F. Wenjun, W. Zhengke, Carbohydrate Polymers.**294**, 119824, (2022)<https://doi.org/10.1016/j.carbpol.2022.119824>.

UNDER PEER REVIEW